Joining Movement Sequences: Modified Dynamic Movement Primitives for Robotics Applications Exemplified on Handwriting

Tomas Kulvicius, KeJun Ning, Minija Tamosiunaite, and Florentin Wörgötter

Abstract—The generation of complex movement patterns, in particular, in cases where one needs to smoothly and accurately join trajectories in a dynamic way, is an important problem in robotics. This paper presents a novel joining method that is based on the modification of the original dynamic movement primitive formulation. The new method can reproduce the target trajectory with high accuracy regarding both the position and the velocity profile and produces smooth and natural transitions in position space, as well as in velocity space. The properties of the method are demonstrated by its application to simulated handwriting generation, which are also shown on a robot, where an adaptive algorithm is used to learn trajectories from human demonstration. These results demonstrate that the new method is a feasible alternative for joining of movement sequences, which has a high potential for all robotics applications where trajectory joining is required.

Index Terms—Delta learning rule, handwriting generation, joining of dynamic movement primitives (DMPs), overlapping kernels.

I. INTRODUCTION

DYNAMIC motion control in robotics requires the accurate production of trajectories and control their dynamic parameters (e.g., position, velocity, and acceleration). Several state-of-the-art methods exist for this. These can be based on splines [1], [2], Gaussian mixture models (GMMs) [3], or dynamic movement primitives (DMPs) [4], to name only some of the most important ones. Recently, much focus has been directed onto DMPs, and they have been used in many studies [5]–[17]. DMPs are units of actions that describe a particular movement trajectory and are formalized as stable attractor systems [4], [18]–[20]. Such movement primitives can be used to generate a movement trajectory either in joint or task space. One observes that DMPs are robust to perturbations, allow for generalization of the trajectory, and also allow for learning. Only few attempts exist that address the problem of DMP joining [7], [14], [15]. Here, we present a modification of the original DMP formulation, and a novel method for joining of movement sequences based on overlapping kernels. The novel method allows us to apply such DMPs to very complex trajectories and to also address the problem of dynamically joining them, which is the main novel contribution of this study.

Humans are able to perform complex movement sequences, e.g., in a manual construction task, in a highly elegant and dynamic fashion. Robots begin to become as dexterous, too. However, the problem to accurately combine trajectories and control position and velocity, which exists in many dexterous robotics applications still leaves many questions open, in particular, when one wants to do this in a dynamic and perturbation-resistant way. We use human handwriting as our test bed. Although in handwriting accuracy at the joining point might not be so important because of "co-articulation," i.e., the next letter is started before the previous one is not completely finished, we have nonetheless chosen it as a useful and complex example. Consider, e.g., signatures. Those are not only defined in position space but also in velocity space, and modern biometric signature recognition makes use of this [21]. In Fig. 1(a), we show three samples of signatures from the same person. One can see that although all three signatures are slightly different, the corresponding velocity profiles [see Fig. 1(b)] have highly similar patterns. How can such complex dynamic profiles be generated in a simple, robust, and generalizable way? We solve this problem by presenting a novel method for joining movement sequences, which can be also applied for other potential uses, especially where precision at the joining point would be crucial, e.g., for grasping and lifting an object.

In the following, we will first describe the formalism for DMP modification and our novel joining approach. One goal here is to provide a powerful but simple method. Then, we will compare our approach with a basic DMP system. We want to strongly emphasize that this comparison is not made to devalue the old approach, but rather to show that the new approach can perform equally well that additionally allows us to join

T. Kulvicius, K. Ning, and F. Wörgötter are with the Department for Computational Neuroscience, III Physikalisches Institut—Biophysik, Bernstein Center for Computational Neuroscience, Georg-August-Universität Göttingen, Göttingen D-37077, Germany (e-mail: tomas@physik3.gwdg.de; nkjchina@hotmail.com; worgott@physik3.gwdg.de).

M. Tamosiunaite is with the Department for Computational Neuroscience, III Physikalisches Institut - Biophysik, Bernstein Center for Computational Neuroscience, Georg-August-Universität Göttingen, Göttingen D-37077, Germany, and also with the Department of Informatics, Vytautas Magnus University, Kaunas 3006, Lithuania (e-mail: m.tamosiunaite@if.vdu.lt).
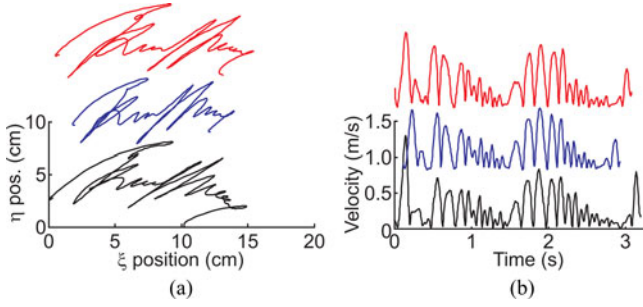
Fig. 1. Three samples of signatures signed by the same person. (a) Position profiles and (b) corresponding velocity profiles. [Here, we show velocities as defined in (14).]

Fig. 2. Modification of the original DMP system. (a) Goal functions r and (b) functions v are shown for the exponential decay system (original DMPs) and the sigmoidal decay system (modified DMPs). The following parameters were used: $g = 10$, $\alpha_g = 0.1$, $T = 75$, $\alpha_v^e = 0.1$, and $\alpha_v^s = 1.0$. For more details, see Section II-A.

movement sequences in a smooth and accurate way. To make this very clear, we will, in Section IV, try to provide a scholarly and fair comparison of some of the existing DMP methods.

II. METHODS

A. Modification of Original Dynamic Movement Primitives

The original DMP system is formalized by second- or third-order differential equations and consists of two dynamic systems: the transformation system and the canonical system [4], [8], [18], [22]. Here, we will use the third-order system since it more closely relates to our modifications. The transformation system is described as follows:

$$\tau \dot{z} = \alpha_z \left(\beta_z \left(r - y \right) - z \right) + f \tag{1}$$

$$\tau \dot{y} = z \tag{2}$$

$$\tau \dot{r} = \alpha_g \left(g - r \right) \tag{3}$$

where g is a known goal state (end point); α_z, β_z, and α_g are time constants; τ is a temporal scaling factor (in this study, we used $\tau = 1$); and $\dot{z}$, $\dot{y}$, and y correspond to the acceleration, velocity, and position, respectively. Here, r defines the delayed goal function.

The canonical system is described by an exponential decay term

$$\tau \dot{v} = -\alpha_v^e \, v \tag{4}$$

where α_v^e is a time constant. The nonlinear function f is given by

$$f = \frac{\sum_{i=1}^{n} \psi_i \, w_i \, v}{\sum_i \psi_i} \left(g - y_0 \right) \tag{5}$$

with

$$\psi_i = e^{-h_i \, (v - c_i)^2} \tag{6}$$

where ψ_i denote Gaussian kernels, h_i is the width of the ith kernel, c_i denotes centers of the kernels, w_i denotes weights, and n denotes number of kernels. Here, $(g - y_0)$ is the scaling term, which guarantees proper scaling when the start or the end point is changed. For more details, see [8]. In addition, coupling terms, such as a phase stopping, can be added to the
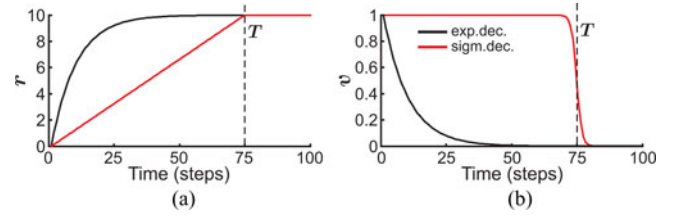
DMP system. In this case, one would need to replace (4) with the following equation as suggested in [8]:

$$\tau \dot{v} = -\frac{\alpha_v^e \, v}{1 + \alpha_c (y_{\text{desired}} - y_{\text{actual}})^2} \tag{7}$$

where α_c is a time constant and defines the strength of the phase stopping. The implications of systems with or without phase stopping will be addressed in Section IV. Here, if not mentioned differently, we are going to use (4).

In order to apply our new joining method using overlapping kernels, we modify the original DMP system by changing the delayed goal function r and the exponential decay function v (see (3) and (4) and Fig. 2). The nonlinear goal function r is replaced by a piecewise linear function and formalized as follows:

$$\tau \dot{r} = \begin{cases} \dfrac{\Delta_t}{T} \, (g - s), & \text{if } t \leq T \\ 0, & \text{otherwise.} \end{cases} \tag{8}$$

Here, s and g define the start and end points of the movement trajectory, respectively; T is the duration of the movement; and Δ_t is the sampling rate. In this study, we used $\Delta_t = 5 \, \text{ms}$, which corresponds to 200 Hz and is consistent with the sampling rate of the pen tablet used for the recordings.

Instead of the exponential decay function, we use a sigmoidal decay function, which is given by

$$\dot{v} = -\frac{\alpha_v^s \, e^{\frac{\alpha_v^s}{\Delta_t} (\tau T - t)}}{\left(1 + e^{\frac{\alpha_v^s}{\Delta_t} (\tau T - t)} \right)^2} \tag{9}$$

where α_v^s defines the steepness of the sigmoidal function centered at the time moment T.

We also use a slightly different nonlinear function f

$$f = \alpha_w \frac{\sum_{i=1}^{n} \psi_i \, w_i \, v}{\sum_i \psi_i} \tag{10}$$

$$\psi_i = e^{-\left(\frac{t}{\tau T} - c_i \right)^2 / 2\sigma_i^2} \tag{11}$$

where σ_i is the width of the ith kernel. Here, kernels are placed evenly along the trajectory in time and spaced between 0 and 1, where 0 and 1 denote, respectively, the beginning and the end of the movement trajectory. The shape of the movement trajectory is defined by weights w_i. To learn the weights, we use the delta rule as explained in Section II-B. Here, we use α_w as a general

scaling factor for all learned weights (note that during learning we always set $\alpha_w = 1$), and in this study, if not specifically mentioned, after learning we also set it to 1. For the influence of α_w on the movement trajectory, see Fig. 4(d)–(g).

The modified system will reach the end point g of the movement trajectory y in time $T + \lambda$ (usually $\lambda \ll T$) with a given accuracy $|g - y(t)| \leq \varepsilon$, where λ depends on the steepness α_η^s, the center point of the sigmoidal function (9), and the movement trajectory itself, i.e., depending on how far one is from the target point at the end T of the movement, the additional time of arrival λ at the target may vary. This strongly depends on how well the nonlinear function f fits the target trajectory. If it fits well, then the trajectory might arrive at the target within little additional time. Otherwise, the additional time that is required could be considerable, such that one cannot always ensure reaching the target at a specific time.

In the original DMP system, the exponential function [see (4)] acts as a phase, as well as a weight scaling variable. In our modified DMP system, the sigmoidal function [see (9)] acts only as a weight scaling variable as our DMP system operates on a scalable time axis. In Section IV, we discuss the differences between a phase-defined or a time-defined DMP system because advantages and disadvantages of the different formulations are not easily discernible.

B. Trajectory Learning

The shape of a trajectory in the DMP system is parameterized by Gaussian kernels ψ_i and their corresponding weights w_i. Several methods exist for weight adaptation in order to learn a target trajectory, such as locally weighted regression methods [4] or global regression methods [14]. As learning is not in the focus of this study, here, we just used the delta learning rule as in artificial neural networks [23], where the error between the target signal and the system's output is used to modify the weights. This rule is simple, but serves our purposes. It can be formalized by the following equation:

$$\Delta w_i^j = \mu \left[\gamma(k) - y^j(k) \right] \tag{12}$$

where γ is the target trajectory (training trajectory), y is the system's output, μ is the learning rate, and k defines the center of the ith Gaussian kernel in the time period $t = 0, \ldots, T$, where T is the duration of the training trajectory γ. Here, $j = 1, \ldots, L$, where L is the number of learning iterations. In this study, we used the same training trajectory γ for each training iteration j, but in general, one can use different training trajectories, e.g., from several demonstration examples. In case, we have more than one dimension, then we have to learn weights for each dimension separately (e.g., for x and y positions in a 2-D case), which can be done independently and in parallel. Note that, here, we learn weights in position space as acceleration is noisier compared with the position.

The presented simple learning approach is not optimal for a single training trajectory. It is more suitable for cases, where many different training trajectories are used and this method will then lead to an average trajectory. If desired, any other regression method [or more sophisticated methods, such as locally

weighted projection regression (LWPR)], can be used to learn the kernel weights.

As mentioned earlier, we tested our modified DMPs on trajectories obtained from handwriting. Handwriting samples were taken from one person, where the person was asked to sign, write single letters and couplets (e.g., "ab"). Data were obtained by the use of a pen tablet (Wacom Intuos3 A3 Wide DTP) with a size of 48.8 cm $\times$ 30.5 cm, resolution of 5080 lpi and a sampling rate of 200 Hz.

In order to evaluate the performance of our method and compare it with the original DMPs, we looked at the position and velocity deviations of the learned trajectory from the target (training) trajectory. We calculated the position deviation by

$$d_{pos} = \sqrt{(y_{\xi_t} - y_{\xi_l})^2 + (y_{\eta_t} - y_{\eta_l})^2} \tag{13}$$

and the velocity deviation as

$$\text{vel}_{t/l} = \sqrt{\dot{y}_{\xi_{t/l}}^2 + \dot{y}_{\eta_{t/l}}^2} \tag{14}$$

$$d_{vel} = |\text{vel}_t - \text{vel}_l| \tag{15}$$

where $y_{\xi/\eta}$ and $\dot{y}_{\xi/\eta}$ are the position and velocity, respectively, ξ and η denote two coordinates in 2-D Cartesian space, and indices t and l stand for the target and learned profiles, respectively.

C. Joining of Dynamic Movement Primitives

A simple way to join several DMPs is to perform one DMP until it reaches the end point and, then, to start the next DMP at that point (in the text, we will call this *simple joining*), i.e., to use the end point of the first DMP as the start point of the second DMP. This approach is very simple, but it has some drawback because of the close-to-zero velocities at the end of the movement trajectory in the original DMPs. Here, we propose a novel method for DMP joining, which can solve this problem and lead to natural and smooth transitions. In our approach, we construct a single set of overlapping kernels ψ' that are defined by centers c' and width of kernels σ' for the whole joint trajectory in the following way. We place centers c' along the joint trajectory in time as follows:

$$c_j^i = \begin{cases} \dfrac{T_1 (i-1)}{T' (n-1)}, & \text{if } j = 1 \\ \dfrac{T_j (i-1)}{T' (n-1)} + \dfrac{1}{T'} \displaystyle\sum_{k=1}^{j-1} T_k, & \text{otherwise} \end{cases} \tag{16}$$

$$c' = c_1^1, c_1^2, \ldots, c_1^n; c_2^1, c_2^2, \ldots, c_2^n; \ldots; c_m^1, c_m^2, \ldots, c_m^n. \tag{17}$$

Here, $i = 1, \ldots, n$ and $j = 1, \ldots, m$, where n is the number of kernels for one DMP and m defines the number of DMPs, and T_k is the duration of the kth DMP. $T' = \sum_{k=1}^{m} T_k$ is the duration of the joint trajectory. We define the width of kernels σ' by

$$\overline{\sigma}_j^i = \frac{\sigma_j^i T_j}{T'} \tag{18}$$

$$\sigma' = \overline{\sigma}_1^1, \overline{\sigma}_1^2, \ldots, \overline{\sigma}_1^n; \overline{\sigma}_2^1, \overline{\sigma}_2^2, \ldots, \overline{\sigma}_2^n; \ldots; \overline{\sigma}_m^1, \overline{\sigma}_m^2, \ldots, \overline{\sigma}_m^n \tag{19}$$
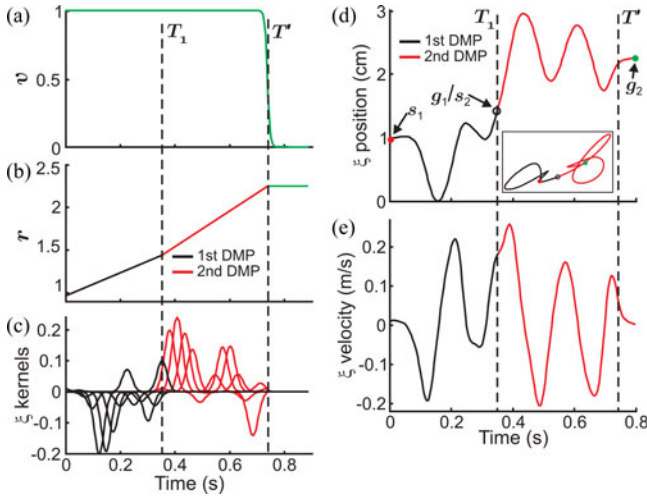
Fig. 3.   DMP joining method with overlapping kernels. Here, we show only signals for the ξ profile of joining two letters "a" and "b." (a) Sigmoidal decay function v, (b) goal function r, (c) kernels ($\psi'_i w'_i v$), and (d) ξ position (y_ξ). In the inset, we show the trajectory of the joined "a" and "b," and (e) ξ velocity ($\dot{y}_\xi$).

where we scale the width of kernels σ^i_j of each DMP with respect to the duration of the joint trajectory T'. Corresponding weights w' for kernels ψ' are obtained from the learned weights w^i_j of each DMP j:

$$w' = w^1_1, w^2_1, \ldots, w^n_1; w^1_2, w^2_2, \ldots, w^n_2; \ldots; w^1_m, w^2_m, \ldots, w^n_m. \tag{20}$$

Finally, we describe the goal function r' by the following equation:

$$\tau \dot{r}' = \begin{cases} \dfrac{\Delta_t}{T_j}(g_j - s_j), & \text{if } \sum_{k=1}^{j-1} T_k \le t \le \sum_{k=1}^{j} T_k \\ 0, & \text{otherwise} \end{cases} \tag{21}$$

where $j = 1, \ldots, m$. We use the same equation for the sigmoidal decay function as given in (9), only here, we use T' instead of T. This way, we construct a more "complex" DMP from several "simpler" DMPs. A graphical illustration of this DMP joining method is shown in Fig. 3, where we show signals that are obtained from joining two letters "a" and "b."

The joining method is designed in such a way that one can control time of the whole joint DMP by setting T' and spatial stretching and squeezing by setting g_j and s_j [see (21)]. Note, similar to conventional DMPs, one can also join our DMPs in a "reactive" way. To do so, one has to set start and end points for the new joint DMP [see (21)] and recalculate kernel parameters (c', σ', and ω') as soon as it is known that a new DMP will be triggered. Then, one continues with the new DMP by the use of (1), (2), (9)–(11), and (21) with the new parameters. If one knows early that a new DMP is triggered (e.g., in the middle of the currently executed DMP), then there will be no differences at the joining point as compared with "nonreactive" (preplanned) joining. If we join the next DMP when the current one is almost finished (around the joining point T_j), then there will be a slow-down in the velocity profile (similar to conventional DMPs).

III. RESULTS

A. Learning and Generalization

An example for trajectory learning is presented in Fig. 4. As a training (target) trajectory, we used a letter "a." The position profile before learning, the position profile, and corresponding kernels for ξ and η positions after 100 learning iterations are, respectively, shown in panels (a)–(c). We can see that initially the system generates more or less a linear trajectory from the start point (red dot) to the end point (green dot), whereas during learning the weights adapt in such a way that after learning we obtained a trajectory that is almost identical to the training trajectory.

To show how well our model can generalize, we made an experiment, where we tested the response of the model after learning when the end point of the movement trajectory was changed. In the first case, we set the end point closer to the start point as compared with the target trajectory; in the second case, the end point was moved further away from the start point. In Fig. 4(d) and (e), we show movement trajectories when the weight scaling factor α_w [see (10)] was set to 1 (no scaling). In this case, we obtain a squeezing (d) or stretching (e) effect compared with the original trajectory. If we use a scaling factor that is proportional to the relation between start and end points of the training and test trajectories (for equation see the caption to Fig. 4), then we get a scaling of the original trajectory that leads either to a smaller (f) or bigger letter "a" (g). The scaling effect presented in panels (f) and (g) is similar to the scaling that is used in the original DMPs [8] (data not shown). Clearly, choosing α_w would depend on the particular application, and further, in this study, we will always use $\alpha_w = 1$.

To get a better feeling for the dynamic reshaping and generalization, Fig. 5(a) shows a comparison between a human signature and a signature that is generated by our modified DMPs. Here, as in the previous case, we show results after 100 learning iterations; however, in this case, narrower kernels were used (for parameters, see the caption of Fig. 5). We can see that trajectories of both signature shapes (left) and corresponding velocities (right) are almost identical as can be judged by the very small errors that are shown in the position and velocity deviation curves [see the lower panels in Fig. 5(a)]. In Fig. 5(b)–(e), we present results of the model for stretching (b), squeezing (c), and for the two cases of diagonal skewing (d) and (e) to give an impression: How the new model generalizes when positions of the start and end points are changed? The velocity profiles that are shown on the right-hand side remain almost identical for panels (b)–(e) showing that the dynamics of the changed signatures remain the same. We have also implemented our method on a simple robotic manipulator platform (Neuro-Robotics, Sussex, U.K.) in our laboratory, letting the robot sign. The resulting trajectory[1] is shown in Fig. 5(f) [compare with the signature shown in panel (a)]. Note that we scaled the output of the system in space and time in order to implement it on the robotic platform.
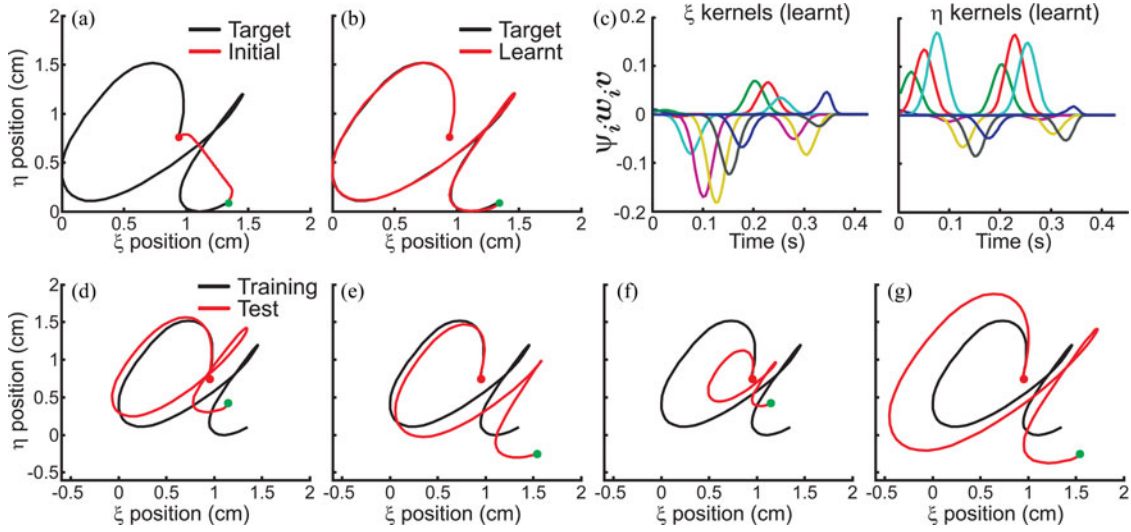
[1]See the supplementary video.

Fig. 4. Results of trajectory learning by the use of the modified DMPs (sigmoidal decay system). (a) Trajectories before learning and (b) and (c) trajectories and kernels ($\psi_i w_i v$) for ξ and η position profiles after learning. Initially, all weights were set to 0.01. (d)–(g) Examples of generalization when different end points are used. (d) and (e) Trajectories without weight scaling ($\alpha_w = 1$) and (f) and (g) with weight scaling, i.e., $\alpha_w = |(g_t - s_t)/(g_l - s_l)|$ (similar to the weight scaling used in the original DMP system [8]), where s_l and g_l denote the start and end points of the training trajectory that is used for learning and s_t and g_t are the start- and end points of the test trial. The following system parameters were used for all cases: number of kernels $n = 15$, width of kernels $\sigma_i = 0.05$, $i = 1, \ldots, n$, number of learning iterations $L = 100$, and learning rate $\mu = 0.1$. Red and green dots represent, respectively, the start and end points of the movement trajectory.

B. Original Versus Modified Dynamic Movement Primitives

A comparison between both systems, i.e., original and modified DMPs, is shown in Fig. 6 [for statistics see Fig. 8(a) and (b)]. Here, we trained both systems with the letters "a" and "b." Results obtained with the original DMPs are shown in panels (a) and (c). We can see that in both cases, the original DMPs can follow the target trajectories very well. We can also observe the drawback of the original DMPs, which is a relatively long and shallow tail of the velocity profile [see panels (a3) and (c3)]. This means that the velocity decays slowly at the end of the movement until the end point of the trajectory is reached. In comparison, results for the modified DMPs (sigmoidal decay system) are shown in panels (b) and (d), where one can see that, as in the original DMPs, we can also reproduce trajectories very well. We note that modified DMPs reach the end-point earlier compared with the original DMPs.[2] This is because of the fact that we use a steep sigmoidal function at the end point of the movement trajectory, which results in quicker convergence to the goal. In our approach, we obtain bigger errors compared with the whole trajectory only at the end of the movement trajectory [see panels (e1) and (f1)] because of the suppressed influence of the kernels by the sigmoidal function, which is necessary to assure convergence to the end point. We observe that we can reproduce not only the position but also the velocity profile [see panels (b3) and (d3)]. Here, we get a relatively large error at the end of the trajectory, and this is because of the fact that here humans lift the pen, whereas our system always stops at the end of the trajectory. In addition, in the modified approach, we have a much quicker velocity decay at the end of the movement compared with the original DMPs (compare a3 with b3 and c3 with

[2]Here, we stopped the system as soon as it reached an accuracy of $\varepsilon = 0.1$ mm with respect to the end point.

d3). In general, we observe that modified DMPs can compete with original approach very well with respect to position and velocity accuracy [see panels (e) and (f)].

C. Joining of Dynamic Movement Primitives

A comparison between the simple joining method that is based on original DMPs and joining with overlapping kernels that is based on modified DMPs is shown in Fig. 7. Here, we show the joining of two letters "a" and "b," where samples "a" and "b" were obtained from a handwritten couplet "ab" by splitting it apart. Systems were trained separately with letters "a" and "b" in order to obtain two DMPs, and then, these DMPs were joined by the use of one joining method or the other. Note that in the simple approach, we start a new DMP at time moment T_1, i.e., when the first DMP is supposed to finish according to the training trajectory. As mentioned earlier, accuracy at the joining point depends on the overlap of the kernels at that point. To investigate this, we varied the number of kernels n and the width σ and analyzed trajectories. In comparison, we also show results for different kernel parameters by the use of original DMPs. Results for four different cases are shown in Fig. 7 (parameters are given in the caption), where in (a), we show results for the simple joining method and in (b) for the new approach. We observe that the usage of more kernels leads to better accuracy at the joining point for both approaches and that the new method is more accurate at the joining point as compared with the simple approach, especially, with respect to the velocity profile. In the following, we will discuss the influence of kernel overlap at the joining point on the accuracy at that point for our new method. In panel (b1) we show position and velocity profiles, where we used few but relatively wide kernels ($n = 10$, $\sigma = 0.1$). One can see that although the transition between two letters is relatively smooth, position and velocity accuracy is much
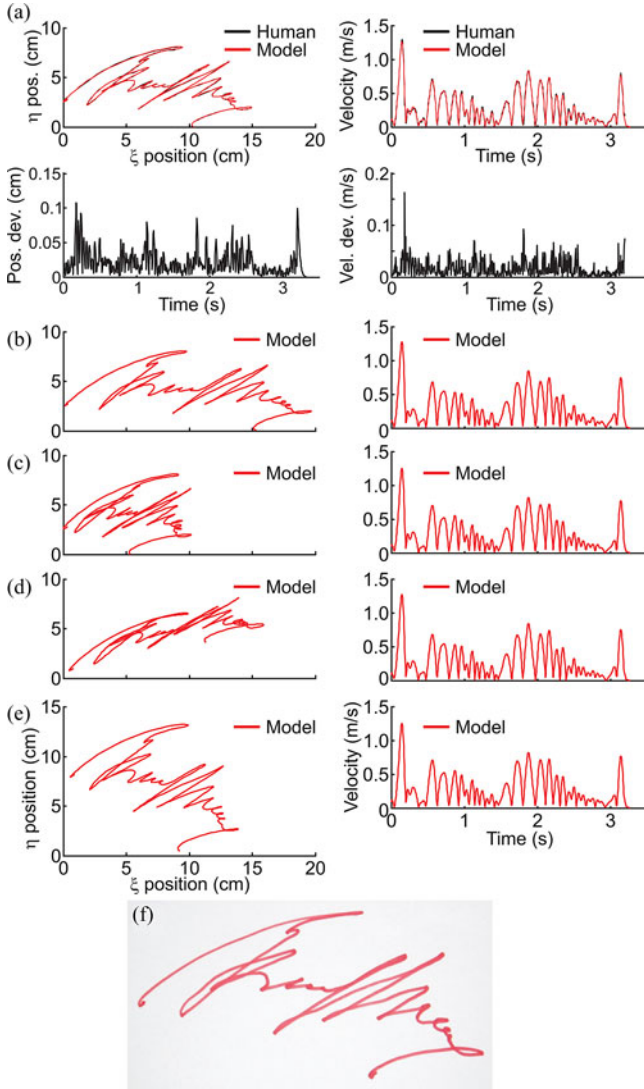
Fig. 5. (a) Comparison of signatures that are signed by a person and generated by the model (modified DMPs). Position profiles (top left), corresponding velocity profiles (top right), position deviation (bottom left), and velocity deviation (bottom right) are shown. These have been obtained by the use of (13) and (15). (b)–(e) Signatures that are generated by the model when different start and end points were used, which correspond to horizontal stretching and squeezing and diagonal skewing. Position profiles (left) and corresponding velocity profiles (right) are shown for each case. (f) Signature that is performed by the robot [compare with the case that is shown in panel (a)]. The following system parameters were used: number of kernels $n = 100$, width of kernels $\sigma_i = 0.01$, $i = 1, \ldots, n$, number of learning iterations $L = 100$, and learning rate $\mu = 0.1$.

worse as compared with the case when more narrower kernels ($n = 15$, $\sigma = 0.05$) are used as shown in panel (b2). If we use even narrower kernels [$n = 30$, $\sigma = 0.015$; see panel (b3)] as compared with the case in panel (b2), we can achieve better accuracy with respect to both position and velocity profiles; however, this can lead to small jerks in the velocity profile (see the inset in panel (b3), bottom) because of such overly slim kernels. One can improve smoothness of the velocity by increasing the width of the kernels as shown in panel (b4), but this might lead to bigger inaccuracy at the joining point in the position profile because of larger overlap at this point.

Position and velocity deviations at the junction point for both approaches are given in Table I. In general, one can see that the new method performs better with respect to the accuracy at the joining point as compared with the simple method. Concerning the new approach, we can summarize that more kernels lead to better accuracy, but if kernels are too narrow, this might produce jerky velocity profiles, whereas if kernels are too wide, this might lead to bigger inaccuracies at the joining point.

D. Statistical Evaluation

We have also performed a statistical evaluation of our system's performance in order to compare it with the original DMPs. First of all, we compared the performance of both systems on single letter experiments as presented in Fig. 6. For this, we used all handwritten letters from the english alphabet, except "i", "j," and "t" (in total 23 letters). These letters were not included in the statistics because of an additional dimension (pen up/down). We looked at the position and velocity deviations (i.e., d_{pos}, d_{vel}) from the target trajectory at specific time points along the movement trajectory. Results of such experiments are shown in Fig. 8(a) and (b) and are consistent with the results shown in Fig. 6. We get similar performance along the whole trajectory for both systems except at the end of the movement, where the modified DMP system has smaller deviations around the time, where the movement is supposed to finish, which leads to faster convergence compared with the original DMPs [see panel (a)]. Concerning velocities [see panel (b)] there are no significant differences and both systems perform equally well except for the fact that modified DMPs have faster velocity decay at the end of the movement [see also Fig. 6(a3), (b3), (c3), and (d3)].

Results for the statistical evaluation of the joining methods are presented in Fig. 8(d) and (e). For the statistics, we used 20 different couplets as shown in Fig. 8(c) and the same procedures as explained in Section III-C. Here, we compare the position and velocity deviations of joint DMPs at their junction point from the target junction point (denoted by the red dot). As demonstrated previously in Fig. 7, we observe that the new joining method produces significantly smaller errors at the joining point than the simple approach with respect to both position and velocity. We also see that accuracy at the joining point depends on the overlap of the kernels and can be improved by increasing the number of kernels. Note that many too wide kernels might lead to worse accuracy in the position profile because of large overlap of kernels at the joining point [see case $n = 30$, $\sigma = 0.03$ in panel (d)].

E. Handwriting Generation

Finally, we applied the novel DMP joining method to the problem of generating handwriting. For this, we trained the system on separately written letters as shown in Fig. 9(A). In this case, we used samples with loops in order to avoid overlapping letters when joining DMPs. After that, we let the system to generate three words: "dmp", "demo," and "norway" (where two of the authors had gone fishing together). Position and corresponding velocity profiles that are generated by the system for the first two words are shown in Fig. 9(b)–(f), where we
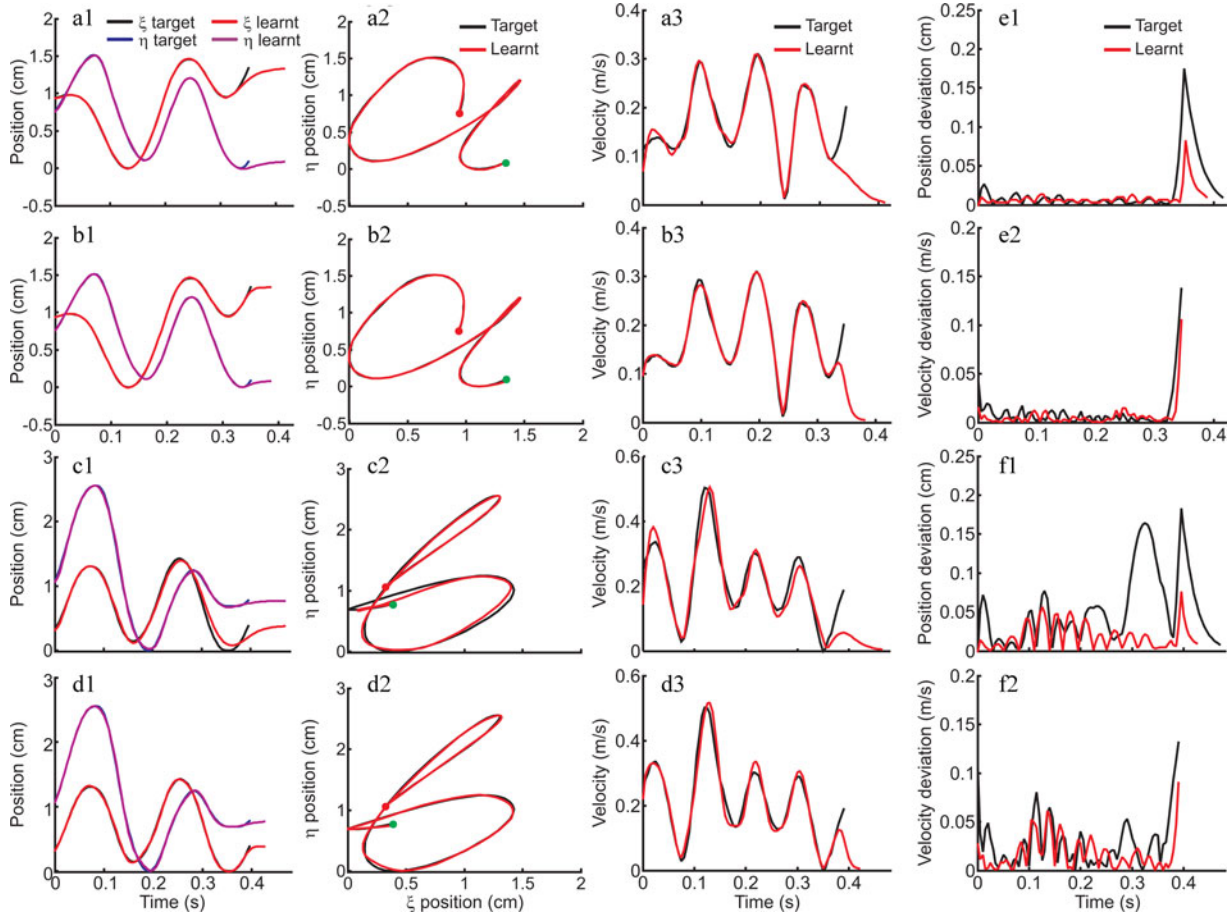
Fig. 6. Comparison between original DMPs (exponential decay system) and modified DMPs (sigmoidal decay system) for letters "a" and "b". (a) and (c) Results for the exponential decay system. Here, we used α_v^s such that the exponential decay function is 95% converged by the time the end-point g is to be reached as suggested in [8]). (b) and (d) Results for the sigmoidal decay system (we used $\alpha_v^s = 1.0$). (a)–(d) ξ and η trajectories plotted over time, position profiles, and the corresponding velocity profiles. Position (13) and velocity (15) deviations for (e1), (e2) the letter "a" and (f1), (f2) the letter "b." The following system parameters were used for both systems: number of kernels $n = 15$, width of kernels $\sigma_i = 0.05$ (for the exponential decay system we tuned h such that it has the same kernel width in time space as for the sigmoidal decay system), and learning rate $\mu = 0.1$. Number of learning iterations L for the exponential decay system was 500 and for the sigmoidal decay system it was 100. Red and green dots represent start- and end-points of the movement trajectory, respectively.

can observe that connections between letters are smooth and natural. As in the previous case, this handwriting generation was also implemented on the robotic manipulator platform[3] and resulting trajectories are shown in Fig. 9(d) and (g). In addition, we also show the system's performance by letting it to generate different handwriting styles for the word "norway." This was done by choosing different end points with respect to the start point and rescaling the start and end points s_j, g_j [see (21)]. Similarly, as already shown for the single letter "a," we get squeezing/stretching/skewing effects of the whole word by setting the end point closer/further away and/or higher/lower with respect to the start point and setting the scaling parameter $\alpha_w = 1$ [words shown in the corners of panel (h)]. If we move the end point further away but set $\alpha_w > 1$, we obtain spatial magnification of the word (corresponds to bigger the font size) and vice versa [see words in the middle of panel (h)], moving the end point closer and setting $\alpha_w < 1$ leads to shrinking of the word (corresponds to smaller font). By doing so, we can see that we retain smooth and natural transitions between the letters.

[3]See supplementary video.

IV. DISCUSSION

In this study, we presented a modification of the original DMP formulation [4], [8], [22] and a novel method for joining several DMPs, which was applied for handwriting generation, as well as implemented, on a robot. Our new method has led to a high accuracy for reproducing complex trajectories and joining movement sequences. We have also statistically evaluated our system's performance and compared it with that of the standard DMPs. In the following, we will discuss our methods in more detail and compare them with other approaches of DMP joining, focusing on a robotics viewpoint. We think, it is clear that handwriting was just chosen as a demonstration scenario and we are neither interested nor will discuss details and implications of handwriting biometry.

In the first part of this study, we proposed a modification of the original DMP formulation in order to apply our new joining method based on overlapping kernels. Here, we made two modifications: 1) instead of the delayed goal function r, we used a piecewise linear goal function [see (3) and (8)] and 2) we replaced the exponential decay function v with a relatively steep
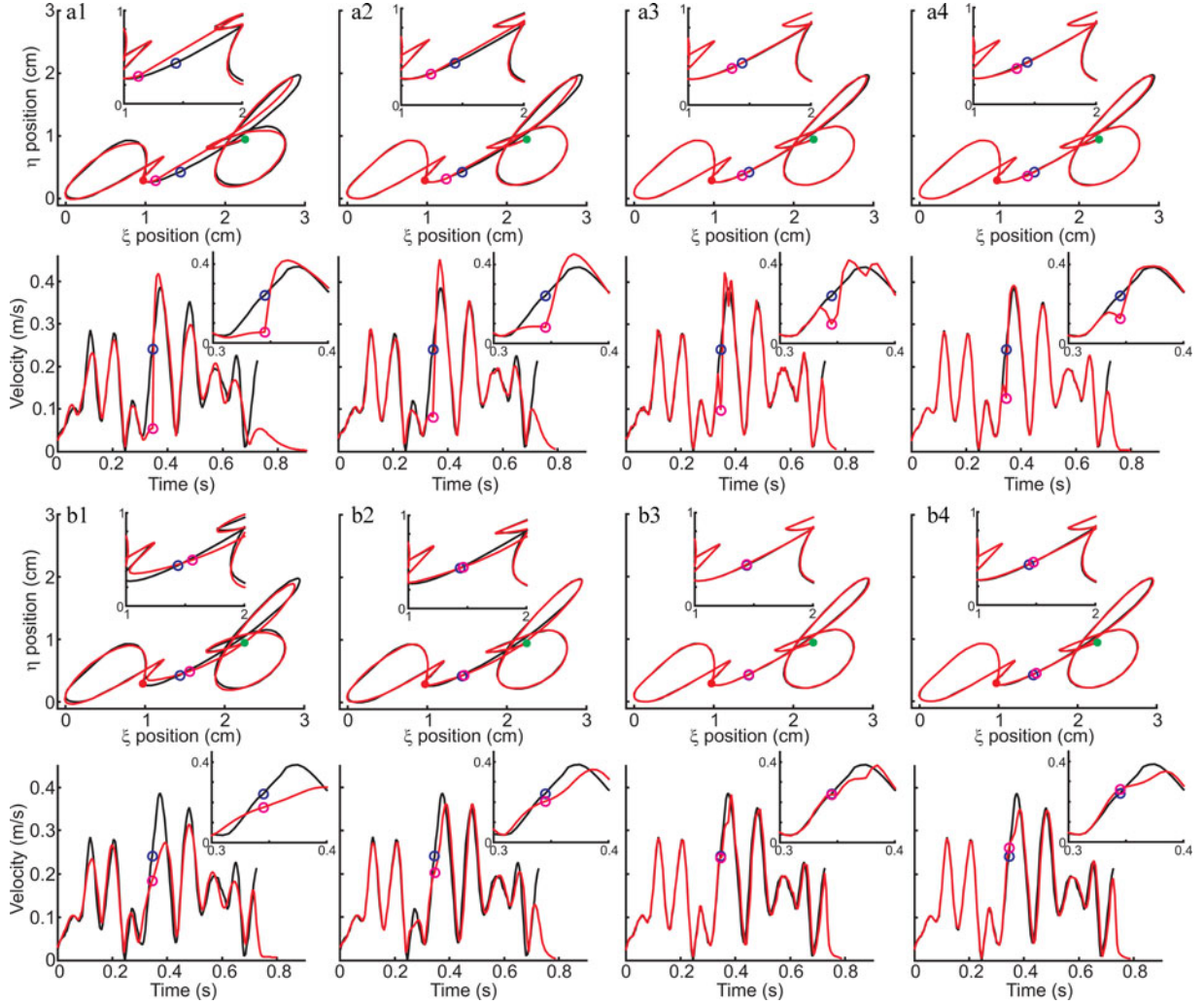
Fig. 7. Comparison between (a) simple DMP joining (exponential decay system) and (b) joining with overlapping kernels (sigmoidal decay system) when using different kernel parameters n (number of kernels) and σ (width of kernels): 1) $n = 10$, $\sigma = 0.1$; 2) $n = 15$, $\sigma = 0.05$; 3) $n = 30$, $\sigma = 0.015$; and 4) $n = 30$, $\sigma = 0.03$. In the top panels, we show position profiles, and corresponding velocity profiles are shown in the bottom panels. In the insets, we show magnified trajectories around the joining point. The same system parameters were used as given in the caption of Fig 6. Red and green dots represent the start and the end point of the movement trajectory, respectively, whereas circles represent the junction points between two DMPs.

TABLE I
DEPENDENCE OF ACCURACY AT THE JOINING POINT ON THE KERNEL
PARAMETERS n (NUMBER OF KERNELS) AND σ (WIDTH OR KERNELS)

		Original DMPs		Modified DMPs	
n	σ	d_{pos} (cm)	d_{vel} (m/s)	d_{pos} (cm)	d_{vel} (m/s)
10	0.100	0.3454	0.1867	0.1366	0.0669
15	0.050	0.2269	0.1601	0.0276	0.0383
30	0.015	0.1002	0.1440	0.0081	0.0036
30	0.030	0.1052	0.1158	0.0464	0.0203

sigmoidal function that is centered at the end point of the trajectory [see (4) and (9)]. These modifications allow reproducing target trajectories with respect to position, as well as velocity profile, while at the same time guaranteeing good convergence to the end point [see Fig. 6(b) and (d)]. Note that we use the linear goal function r together with kernels ψ, which are independent of the function v, i.e., our system is directly dependent on time. (How to alter this will be discussed later in the text.) This makes

our approach more similar to splines, but we have maintained attractive features of original DMPs, such as robustness to perturbations [see Fig. 10(b1) and (b2)] and generalization [see Fig. 4(d)–(g) and Fig. 5(b)–(e)]. We think that such features are very useful and provide some advantages over splines, where they are not immediately present. An unequivocal decision in favor or against any method, however, depends for all these approaches much on the task and sometimes splines might still be a better solution. We also would like to stress that our system is easily scalable with respect to the dynamics of the system (τ) and space without losing the qualitative trajectory appearance that was originally coded in the DMP weights. Depending on the application, two generalization options for the trajectory are possible with our DMPs. In one case, if $\alpha_w = 1$ [see (10)], then we get a stretching or squeezing effect of the learned trajectory when start point and/or end point are changed [see Fig. 4(d) and (e)], whereas when $\alpha_w \neq 1$, we obtain a smaller or larger
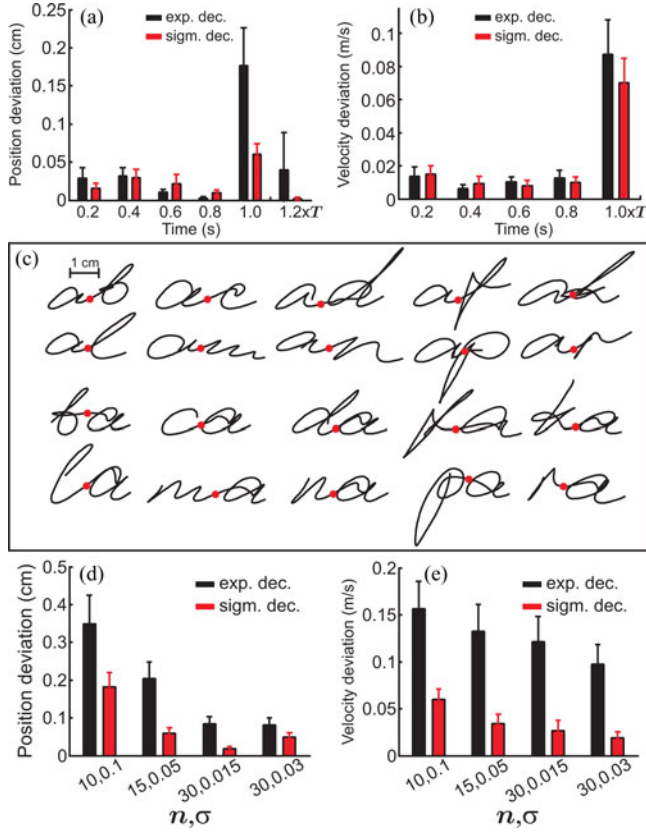
Fig. 8. Statistical comparison between original DMPs (exponential decay system) and modified DMPs (sigmoidal decay system). (a) Average position deviation d_{pos} and (b) velocity deviation d_{vel} obtained from 23 letters. Statistical comparison between joining with the simple method based on original DMPs and the joining method with overlapping kernels based on modified DMPs when using different kernel parameters n (number of kernels) and σ (width of kernels). (c) Twenty couplets used for the statistical evaluation shown in panels (d) and (e). Red dots denote the junction points. (d) Average position deviation d_{pos} and (e) velocity deviation d_{vel} computed at the junction points as shown in panel (c). Here, error bars denote confidence intervals of the mean (95%). The same system parameters were used as given in the caption of Fig. 6.

position profile (see Fig. 4(f) and (g), similar to scaling that is proposed in [8]).

As already mentioned in Section I, several methods exist for trajectory generation, e.g., those based on splines, DMPs, or GMMs. In the following paragraph, we will discuss the behavior of different types of DMPs for some specific cases and at the end compare those also with results from the literature that is obtained with GMMs. Differences will emerge, but before discussing those, it is important to note that the now following comparison should not be used to deduce quality assessments of the different methods. Many times the actual quality of a method depends critically on the task and a method that performs badly under some conditions can be superior under different ones. Thus, fair comparisons are difficult if not impossible. Still we think that the behavior displayed in Fig. 10 might be helpful to appreciate and understand the similarities and differences of the shown methods.

Original DMPs are designed in such a way that they are not directly dependent on time, which allows adding coupling terms or phase resetting techniques [8]. By replacement of time with a
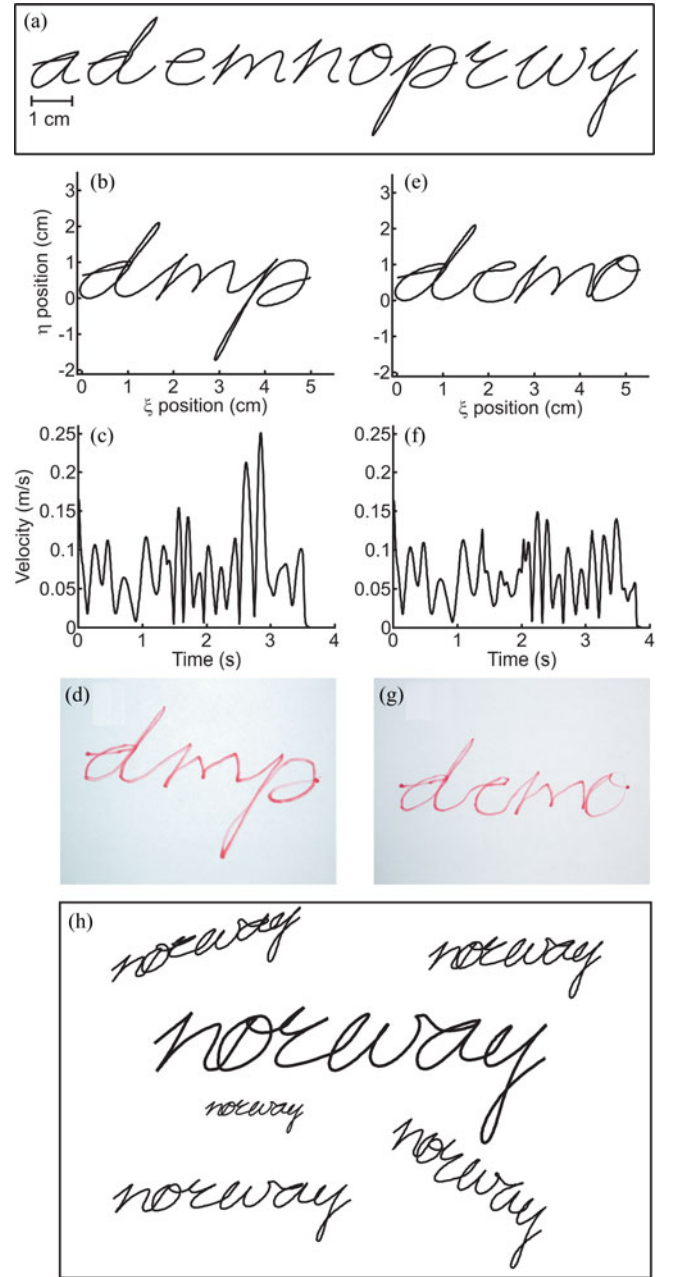

Fig. 9. Results of handwriting generation using modified DMPs (sigmoidal decay system). (a) Samples of single letters used to generate the words "dmp" [panels (b)–(d)], "demo" [panels (e)–(g) and "norway" [panel (h)]. (b), (e) Position profiles. (c) and (f) Corresponding velocity profiles generated by the modified DMP system. (d) and (g) Trajectories of handwriting produced by the robot. (h) Example of different handwriting generation by changing end points (simulation results). The same system parameters were used as given in the caption of Fig. 6.

phase variable, one can manipulate the time evolution of phase, i.e., by slowing down or speeding up the movement as appropriate. One example of such a coupling is *phase stopping,* which prevents the actual trajectory from moving too far away in the case of a perturbation [8]. In Fig. 10(a1) and (a2), we show the behavior of original DMPs in the case of a perturbation without [see (4)] and with phase stopping [see (7)], respectively. Indeed, we can see that DMPs with phase stopping behave
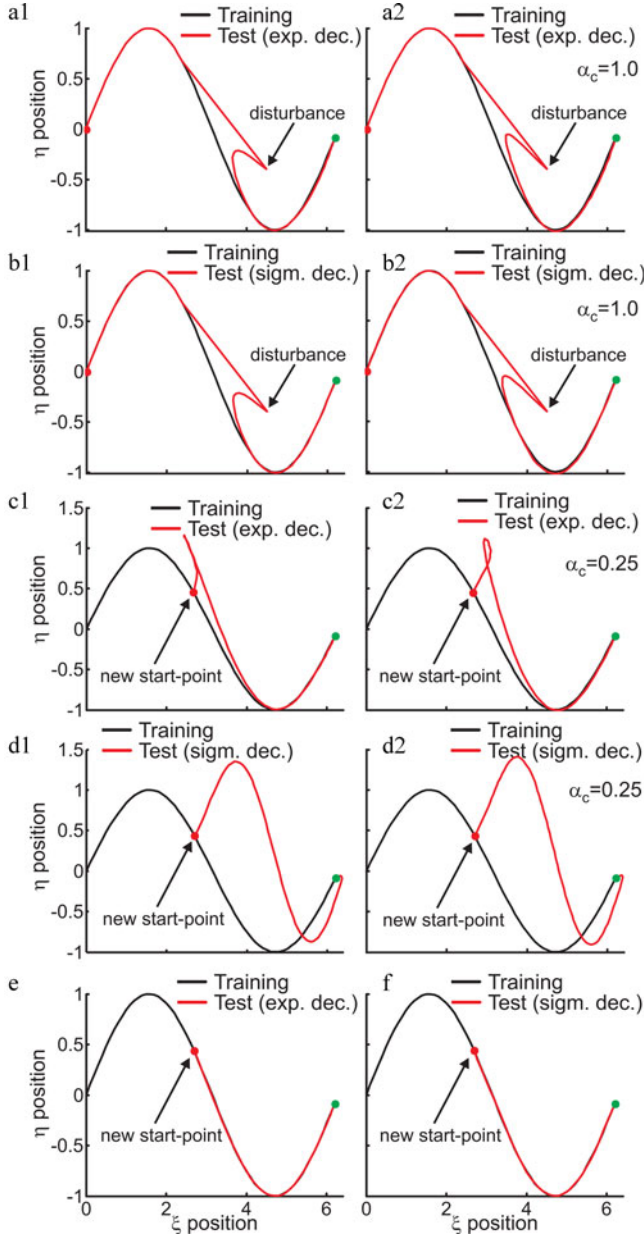
Fig. 10. Comparison between (a), (c), (e) original (exponential decay system) and (b), (d), (f) modified (sigmoidal decay system) DMPs. (a)–(d) Results without phase stopping (left) and with phase stopping (right) [see (7) and (22)]. (a) and (b) Performance of different DMP systems when a disturbance is applied. We disturbed the system by $\Delta y_\xi(t) = \Delta y_\xi(t) + 2$ and $\Delta y_\eta(t) = \Delta y_\eta(t) - 1$ at the time moment $t = 0.4T$. (c)–(f) Performance when the start point is changed, where in case (e), a phase cut and in case (f), a time cut was applied at the new start point. Note that in cases (c1), (c2), and (e), we used (5) without scaling $(g - y_0)$ in order to make it comparable with modified DMPs. Other system parameters were as given in the caption of Fig. 6. Only in this case, we used 30 kernels with width $\sigma = 0.025$.

differently compared with DMPs without phase stopping by pushing the trajectory more toward the perturbation point. Note that this example was specifically chosen to show this particular effect and the response characteristics of the system might be to some degree different for different perturbations at other times. The effect of phase stopping in this example is significant but not very strong and more time will be required to allow for

this compensation to happen, i.e., this makes the time of the movement execution longer. We can also extend our approach by adding the phase variable in order to make it not directly dependent on time and obtain phase stopping. This can be done by the following equations. Let us add an additional phase variable

$$\tau \dot{\theta} = \frac{\Delta_t}{1 + \alpha_c (y_{\text{desired}} - y_{\text{actual}})^2} \qquad (22)$$

with $\theta_0 = 0$ and replace (8) by

$$\dot{r} = \begin{cases} \dot{\theta}\,(g - s)/(T), & \text{if } \theta \leq T \\ 0, & \text{otherwise.} \end{cases} \qquad (23)$$

In doing this, we also need to replace, everywhere, the time variable t with the phase variable θ. As demonstrated in Fig. 10(b1) and (b2), we can see that the modified DMPs behave similarly to the original method.

In a second set of experiments, we compared the behavior of the systems when the start point is moved further away along the trajectory as compared with the training trajectory. With this we want to compare generalization properties of the different systems. Results of such experiments are shown in Fig. 10(c)–(f), where a different behavior is observed for the original DMPs (with and without phase stopping) as compared with the modified DMPs [compare panels (c1), (c2), and (d1), (d2)]. In case (c1), the system first of all tries to go back to the originally trained start point and only later continues to follow the target (training) trajectory, whereas phase stopping (c2) prevents the system from going backward. The behavior of our modified DMPs is presented in panels (d1) and (d2), where a squeezing effect of the original trajectory is observed in both cases. Here, the phase stopping has no effect on the trajectory since our modified system follows the new (squeezed) trajectory and the phase stopping that is caused by the deviation from the training trajectory only slows down the motion process but does not change the shape of the trajectory. Instead of backtracking or squeezing [see panels (c) and (d)], one can also easily obtain a behavior, where the trajectory just begins at the shifted start point [see panels (e) and (f)]. For this, one needs to set appropriate phase (e) or time (f) at the corresponding position.

Another type of attractor-based trajectory generators are GMMs [3], [24]. In GMMs, a movement is described by a nonlinear time-invariant dynamical system, where the convergence to the end point of all trajectories is ensured starting from any point in the target space forming a trajectory-embedding surface, which is obtained by learning from a set of demonstrations (see [24, Fig. 10]). The behavior of GMMs in the case of perturbations much depends on the obtained trajectory-embedding surface, which may vary depending on the used learning method. Therefore, in the case of a perturbation, a GMM might first of all come back to the target (training) trajectory and later continue along the training trajectory or go directly from perturbation point to the end point. In case, the start point is moved further away along the trajectory as compared with the training trajectory, the GMM would continue following the target trajectory directly from the shifted start point (similar to the DMP behavior in Fig. 10(e) and (f), since GMMs are time invariant. Clearly,

choosing a system for movement generation much depends on the task and on which type of behavior is desired. For example, whether it is important to follow the trajectory or reach the goal at a specified time, continue following the trajectory from the new start point or return to the trained start point, and so on.

Several methods exist for the imitation learning of a target trajectory, such as locally weighted regression methods [4], [8], global regression methods [14] or Gaussian mixture regression [25]. For instance, by the use of locally weighted regression, one can learn not only the appropriate weights w_i of the kernels but also the number of kernels n, their centers c_i, and widths h_i, automatically. Here, we used a simpler learning rule to train weights w_i, which is known as the delta learning rule in artificial neural networks [23], which is not optimal for a single training sample (regression methods would succeed in one-shot learning in this case). On the other hand, in our case, position information that is obtained from demonstration is enough for the determination of the DMP weights. We do not have to measure acceleration or velocity (or obtain these by the calculation of derivatives) as required for regression methods in DMP weight learning procedures [8]. Although here we adapt only the weights of the kernels, while leaving their centers and widths fixed, we can still achieve high learning accuracy. In general, we obtained that for trajectories with relatively slow dynamics, like letters, one needs fewer but wider kernels to accurately approximate the trajectory, whereas for relatively complex trajectories with fast dynamics, like signatures, more but narrower kernels are required. Similar to other methods, such a learning procedure would lead to an average trajectory when different training samples are used. Clearly, our simple learning method could be replaced by any of the more advanced approaches (e.g., regression methods), which might be advisable in cases of single training samples or where the dynamics of the trajectory changes strongly "along the way."

Our approach assumes a single reference trajectory and it can generalize quite well for points close enough to this trajectory. Generalization, however, e.g., drops when motion starts/ends at points too far away from this trajectory. For robot tasks that require generalization over a larger domain, one might choose other learning alternatives, such as GMMs, that form a trajectory-embedding surface from a set of demonstrations [3], [24]. In addition, in our setup, we learnt weights along each dimension separately. However, such an assumption of independent dimensions is not generally true for many motions, especially, in the case of perturbations. Depending on the application, one might use other methods, such as *stable estimator of dynamical systems* [24], which is a single multidimensional model and considers correlations across several dimensions.

A classical way to join several trajectories are spline-based solutions [1], [2], which allow joining trajectories smoothly with predefined velocity and/or acceleration. This approach, however, is not an online trajectory generator and lacks attractive features of DMPs, such as robustness to perturbations and generalization. In [26], a motion planner for object manipulation has been proposed, which allows sequencing of actions. In their approach, complex motion is divided into *transit paths* (e.g., approaching an object) that do not move objects and *transfer*

paths that move objects (e.g., grasping and carrying an object). A manipulation is performed by concatenation of alternating sequences of such paths that connect the initial system's configuration to a final (goal) configuration. This is a kinematic approach, where the solution is based on the configuration of manipulators and objects and, different from DMPs, does not consider the dynamics of the movement, i.e., velocities and accelerations.

DMPs have been applied for different robotics applications, such as movement with obstacle avoidance [10], [11], lifting [13], pouring [12], [14], hitting and batting [9], [15], [18], flight control [7], drumming [17], [27], walking [5], [20], and jumping [16]. However, not so much work has been done with respect to joining of DMPs [7], [14], [15]. Therefore, in this study, we were mainly concerned with the problem of joining several DMPs. This was motivated by a drawback of the original DMP system, namely, its velocity profile that produces a relatively long and shallow decay until it reaches the end point. This means that the system has to stop (to reach zero velocity) before a new DMP can be started. To avoid jumps in velocity and acceleration, a simple solution for this problem, as demonstrated in [14], would be to apply a first-order low-pass filter (augment original DMPs to a third-order system). However, if positions and velocities of both DMPs are, at the joining point, too different from each other, one would need to smooth the trajectory a lot, which, as a consequence produces large deviations from the target trajectory because of the delay produced by the first-order filter. Another approach for joining movement sequences that is based on a modification of the original DMPs is introduced by Kober *et al.* [15] for learning of hitting and batting. In this case, the original DMPs are augmented by the introduction of two additional terms, namely, moving target and final boundary velocity. Such a method allows joining several DMPs at a specific position with a predefined velocity. In [7], a method to get smooth transitions has been proposed when joining several DMPs based on partial contraction theory [28]. In their approach, the trajectory of one DMP is forced to converge to the other leading to a smooth transition between two DMPs. In contrast with the presented methods, in our approach, we do not augment the system by the additional equations or terms but simply create one joint DMP by overlapping kernels of several single DMPs. This way, a smooth, natural, and accurate transition, as exemplified on handwriting, emerges from the system itself without a deceleration at the joining point (see Fig. 3). This method inherits the properties of the modified DMPs, such as scalability and generalization, like stretching and squeezing, when start and/or end points are changed as shown in Fig. 9(h). In this case, one only needs to appropriately scale start and end points [s_j and g_j, see (21)] at the joining points. The trajectory around the joining point is dependent on the overlap of kernels [see Fig. 7(b)–(e)] and some tuning would be required in the cases, where high accuracies at the joining point are required.

We believe that the attractive properties of our joining method, such as scalability, generalization, and smoothness, have some potential for different kind of robotics applications. Using robots to actually forge signatures will, however (luckily!), still remain only a possible topic for entertaining science fiction. After all,

it is unlikely that human-like ("android") machines will exist in the next 50 or so years, with an appearance that could deceive a customer clerk and let him/her forget that actually a robot hand is doing the writing.

ACKNOWLEDGMENT

REFERENCES

[1] R. H. Castain and R. P. Paul, "An on-line dynamic trajectory generator," *Int. J. Robot. Res.*, vol. 3, no. 1, pp. 68–72, 1984.

[2] B. Siciliano, L. Sciavicco, L. Villani, and G. Oriolo, *Robotics: Modelling, Planning and Control.* New York: Springer-Verlag, 2009.

[3] S. M. Khansari-Zadeh and A. Billard, "BM: An iterative method to learn stable non-linear dynamical systems with Gaussian mixture models," in *Proc. IEEE Int. Conf. Robot. Autom.*, 2010, pp. 2381–2388.

[4] J. A. Ijspeert, J. Nakanishi, and S. Schaal, "Movement imitation with nonlinear dynamical systems in humanoid robots," in *Proc. IEEE Int. Conf. Robot. Autom.*, 2002, pp. 1398–1403.

[5] J. Nakanishi, J. Morimoto, G. Endo, G. Cheng, S. Schaal, and M. Kawato, "Learning from demonstration and adaptation of biped locomotion," *Robot. Auton. Syst.*, vol. 47, nos. 2–3, pp. 79–91, 2004.

[6] J.-X. Xu, W. Wang, P. Vadakkepat, and L. W. Yee, "ANN based internal model approach to motor learning for humanoid robot," in *Proc. Int. Joint Conf. Neural Netw.*, 2006, pp. 4179–4186.

[7] B. E. Perk and J. J. E. Slotine, "Motion primitives for robotic flight control," Cornell Univ., Ithaca, NY, Rep. cs/0609140, Sep. 2008.

[8] S. Schaal, P. Mohajerian, and A. Ijspeert, "Dynamics systems vs. optimal control—A unifying view," *Prog. Brain Res.*, vol. 165, pp. 425–445, 2007.

[9] J. Peters and S. Schaal, "Reinforcement learning of motor skills with policy gradients," *Neural Netw.*, vol. 21, no. 4, pp. 682–697, 2008.

[10] D.-H. Park, H. Hoffmann, P. Pastor, and S. Schaal, "Movement reproduction and obstacle avoidance with dynamic movement primitives and potential fields," in *Proc. 8th IEEE-RAS Int. Conf. Humanoid Robots*, 2008, pp. 91–98.

[11] H. Hoffmann, P. Pastor, D.-H. Park, and S. Schaal, "Biologically-inspired dynamical systems for movement generation: Automatic real-time goal adaptation and obstacle avoidance," in *Proc. IEEE Int. Conf. Robot. Autom.*, 2009, pp. 1534–1539.

[12] P. Pastor, H. Hoffmann, T. Asfour, and S. Schaal, "Learning and generalization of motor skills by learning from demonstration," in *Proc. IEEE Int. Conf. Robot. Autom.*, 2009, pp. 763–768.

[13] S. Bitzer and S. Vijayakumar, "Latent spaces for dynamic movement primitives," in *Proc. 9th IEEE-RAS Int. Conf. Humanoid Robots*, 2009, pp. 574–581.

[14] B. Nemec, M. Tamosiunaite, F. Woergoetter, and A. Ude, "Task adaptation through exploration and action sequencing," in *Proc. 9th IEEE-RAS Int. Conf. Humanoid Robots*, 2009, pp. 610–616.

[15] J. Kober, K. Mülling, O. Krömer, C. H. Lampert, B. Schölkopf, and J. Peters, "Movement templates for learning of hitting and batting," in *Proc. IEEE Int. Conf. Robot. Autom.*, 2010, pp. 1–6.

[16] E. Theodorou, J. Buchli, and S. Schaal, "Reinforcement learning of motor skills in high dimensions: A path integral approach," in *Proc. IEEE Int. Conf. Robot. Autom.*, 2010, pp. 2397–2403.

[17] A. Ude, A. Gams, T. Asfour, and J. Morimoto, "Task-specific generalization of discrete and periodic dynamic movement primitives," *IEEE Trans. Robot.*, vol. 26, no. 5, pp. 800–815, Sep. 2010.

[18] A. Ijspeert, J. Nakanishi, and S. Schaal, "Learning attractor landscapes for learning motor primitives," in *Proc. 15th Adv. Neural Inf. Process. Syst.*, 2003, pp. 1547–1554.

[19] S. Schaal, "Dynamic movement primitives—A framework for motor control in humans and humanoid robots," in *Proc. Int. Symp. Adaptive Motion Animals Mach.*, 2003.

[20] S. Schaal, J. Peters, J. Nakanishi, and A. Ijspeert, "Control, planning, learning, and imitation with dynamic movement primitives," in *Proc. IEEE Int. Conf. Intell. Robots Syst. Workshop Bilateral Paradigms Humans Humanoids*, 2003.

[21] A. I. Al-Shoshan, "Handwritten signature verification using image invariants and dynamic features," in *Proc. Int. Conf. Comput. Graph., Imag. Vis.*, 2006, pp. 173–176.

[22] S. Schaal, J. Peters, J. Nakanishi, and A. Ijspeert, "Learning movement primitives," in *Proc. Int. Symp. Robot. Res.*, 2004, pp. 561–572.

[23] S. Haykin, *Neural Networks: Comprehensive Foundation.* Englewood Cliffs, NJ: Prentice-Hall, 1999.

[24] S. M. Khansari-Zadeh and A. Billard, "Imitation learning of globally stable non-linear point-to-point robot motions using nonlinear programming," in *Proc. IEEE Int. Conf. Intell. Robots Syst.*, 2010, pp. 2676–2683.

[25] S. Calinon, F. Guenter, and A. Billard, "On learning, representing, and generalizing a task in a humanoid robot," *IEEE Trans. Syst. Man Cybern. B*, vol. 37, no. 2, pp. 286–298, Apr. 2007.

[26] Y. Koga, K. Kondo, J. Kuffner, and J.-C. Latombe, "Planning motions with intentions," in *Proc. 21st Ann. Conf. Comput. Graph. Interact. Tech.*, 1994, pp. 395–408.

[27] S. Schaal, "Movement planning and imitation by shaping nonlinear attractors," in *Proc. 12th Yale Workshop Adapt. Learning Syst.*, 2003.

[28] W. Wang and J. J. Slotine, "On partial contraction analysis for coupled nonlinear oscillators," *Biol. Cybern.*, vol. 92, no. 1, pp. 38–53, 2005.

Tomas Kulvicius received the M.S. degree from Vytautas Magnus University, Kaunas, Lithuania, in 2003 and the Ph.D. degree from the University of Göttingen, Göttingen, Germany, in 2010, both in computer science. His Ph.D. dissertation focused on the development of receptive fields in closed-loop learning systems.

Currently, he is a Postdoctoral Researcher with the Department for Computational Neuroscience, University of Göttingen. His research interests include closed-loop behavioral systems, learning algorithms, receptive fields, robotics, dynamic movement primitives, biosignal analysis, and biological system modeling.
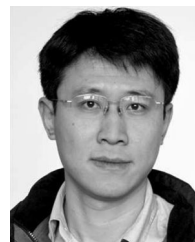
KeJun Ning received the B.S. (Hons.) and M.S. (Hons.) degrees in mechanical engineering from Northeastern University, Shenyang, China, in 1999 and 2002, respectively, and the Ph.D. degree in mechatronics engineering from Shanghai Jiao Tong University, Shanghai, China, in 2006.

From May 2006 to July 2007, he was a Senior Mechatronic System Engineer with Shanghai Grandar Robotics Co. Ltd., China. From August 2007 to May 2008, he was a Senior Engineer and Researcher with the Robotics Department, China Corporate Research Center, Shanghai Branch, ABB (China) Ltd., China. He is currently a Postdoctoral Researcher with the Bernstein Center for Computational Neuroscience, University of Göttingen, Göttingen, Germany. His research interests include the areas of robotics, mechanism design, embedded systems, and autonomous systems.

Minija Tamosiunaite received the Ph.D. degree in informatics from Vytautas Magnus University, Kaunas, Lithuania, in 1997.

Currently, she is working as a Senior Researcher with the Bernstein Center for Computational Neuroscience, Institute Physics III, University of Göttingen, Göttingen, Germany. Her research interests include machine learning, biological signal analysis, and the application of learning methods in robotics.

Florentin Wörgötter studied biology and mathematics with the University of Düsseldorf, Düsseldorf, Germany. He received the Ph.D. degree for work on the visual cortex from the University of Essen, Essen, Germany, in 1988.

From 1988 to 1990, he was engaged in computational studies with the California Institute of Technology, Pasadena. From 1990 to 2000, he was a Researcher with the University of Bochum, Bochum, Germany, where he was involved in the investigation of the experimental and computational neuroscience of the visual system. From 2000 to 2005, he was a Professor of computational neuroscience with the Psychology Department, University of Stirling, Stirling, U.K., where his interests strongly turned toward "learning in neurons." Since July 2005, he has been the Head of the Computational Neuroscience Department, Bernstein Center for Computational Neuroscience, Institute Physics III, University of Göttingen, Göttingen, Germany. His group has also developed the RunBot, which is a fast and adaptive biped-walking robot. His current research interests include information processing in closed-loop perception-action systems, sensory processing, motor control, and learning/plasticity, which are tested in different robotic implementations.